

Adipocyte-specific tribbles pseudokinase 1 regulates plasma adiponectin and plasma lipids in mice



Elizabeth E. Ha¹, Gabriella I. Quartuccia¹, Ruifeng Ling¹, Chenyi Xue¹, Rhoda A. Karikari², Antonio Hernandez-Ono³, Krista Y. Hu¹, Caio V. Matias¹, Rami Imam¹, Jian Cui¹, Natalia S. Pellegata², Stephan Herzig², Anastasia Georgiadi², Rajesh K. Soni⁴, Robert C. Bauer^{1,*}

ABSTRACT

Objective: Multiple genome-wide association studies (GWAS) have identified SNPs in the 8q24 locus near *TRIB1* that are significantly associated with plasma lipids and other markers of cardiometabolic health, and prior studies have revealed the roles of hepatic and myeloid *Trib1* in plasma lipid regulation and atherosclerosis. The same 8q24 SNPs are additionally associated with plasma adiponectin levels in humans, implicating *TRIB1* in adipocyte biology. Here, we hypothesize that *TRIB1* in adipose tissue regulates plasma adiponectin, lipids, and metabolic health.

Methods: We investigate the metabolic phenotype of adipocyte-specific *Trib1* knockout mice (Trib1_ASKO) fed on chow and high-fat diet (HFD). Through secretomics of adipose tissue explants and RNA-seq of adipocytes and livers from these mice, we further investigate the mechanism of *TRIB1* in adipose tissue.

Results: Trib1_ASKO mice have an improved metabolic phenotype with increased plasma adiponectin levels, improved glucose tolerance, and decreased plasma lipids. Trib1_ASKO adipocytes have increased adiponectin production and secretion independent of the known *TRIB1* function of regulating proteasomal degradation. RNA-seq analysis of adipocytes and livers from Trib1_ASKO mice indicates that alterations in adipocyte function underlie the observed plasma lipid changes. Adipose tissue explant secretomics further reveals that Trib1_ASKO adipose tissue has decreased ANGPTL4 production, and we demonstrate an accompanying increase in the lipoprotein lipase (LPL) activity that likely underlies the triglyceride phenotype.

Conclusions: This study shows that adipocyte *Trib1* regulates multiple aspects of metabolic health, confirming previously observed genetic associations in humans and shedding light on the further mechanisms by which *TRIB1* regulates plasma lipids and metabolic health.

© 2021 The Authors. Published by Elsevier GmbH. This is an open access article under the CC BY-NC-ND license (<http://creativecommons.org/licenses/by-nc-nd/4.0/>).

Keywords Adipose; Metabolic syndrome; Lipoproteins; GWAS; Tribbles; Pseudokinases

1. INTRODUCTION

Genome-wide association studies (GWAS) have repeatedly identified SNPs in the 8q24 locus as associated with multiple traits related to cardiometabolic disease, including plasma triglyceride (TG) [1,2], HDL-cholesterol (HDL-C), total cholesterol (TC), LDL-cholesterol (LDL-C) [1–6], coronary artery disease (CAD) [6,7], circulating liver transaminases (ALTs/ASTs) [8], and most recently with HbA1c levels [9]. These SNPs lie ~40 kb downstream of the *TRIB1* gene, which codes for the Tribbles pseudokinase 1 [10], implicating *TRIB1* in numerous facets of metabolism. As a pseudokinase, *TRIB1* lacks the ability to phosphorylate target proteins. Rather, *TRIB1* is best known as a scaffolding protein that facilitates protein–protein interactions leading to the post-translational modification (phosphorylation or ubiquitination) of the target proteins [11]. Subsequent *in vivo* studies confirmed the role of hepatic *TRIB1* in these metabolic phenotypes, as liver-

specific overexpression of *Trib1* in mice decreases plasma cholesterol and TGs [12], whereas hepatic deletion of *Trib1* increases plasma cholesterol and TGs and also increases hepatic steatosis due to elevated *de novo* lipogenesis [13]. Furthermore, myeloid-specific *Trib1* knockout mice have reduced foam cell formation and atherosclerotic burden [14], implicating myeloid *TRIB1* in CAD pathogenesis. These studies highlight the importance of tissue-specific gene functions and raise the question of how much *Trib1* function in other tissues contributes to the GWAS associations.

In addition to the traits listed above, the *TRIB1* GWAS SNPs are also associated with plasma adiponectin levels in humans, with the effect allele associated with a 3% increase in circulating adiponectin [15] (Figure S1). Adiponectin (ADIPOQ) is an adipokine secreted exclusively from the adipose tissue, implicating *TRIB1* in adipose tissue biology. Adiponectin acts predominantly as an insulin-sensitizing agent through signaling to the liver and skeletal muscle [16], while further studies

¹Cardiometabolic Genomics Program, Division of Cardiology, Department of Medicine, Columbia University, New York, NY, USA ²Institute for Diabetes and Cancer, Helmholtz Centre, Munich, Germany ³Department of Medicine, Vagelos College of Physicians and Surgeons, Columbia University, New York, NY, USA ⁴Proteomics and Macromolecular Crystallography Shared Resource, Herbert Irving Comprehensive Cancer Center, Columbia University, New York, NY, USA

*Corresponding author. Columbia University Irving Medical Center, 630 W. 168th Street, PS10-401, New York, NY 10032, USA. E-mail: rcb36@columbia.edu (R.C. Bauer).

Received August 13, 2021 • Revision received November 16, 2021 • Accepted November 30, 2021 • Available online 7 December 2021

<https://doi.org/10.1016/j.molmet.2021.101412>

have linked adiponectin with hepatic fat content [17], decreased plasma TG [18], increased HDL-C [18], decreased NAFLD [19], and decreased risk of CAD [20]. Thus, adiponectin has a beneficial effect on various markers of metabolic health, indicating a therapeutic benefit of increasing circulating adiponectin levels [21]. Adipose tissue is increasingly recognized as a critical regulator of metabolic homeostasis and health, chiefly due to its function in storing TGs through lipoprotein lipase (LPL)-mediated uptake from TG-rich lipoproteins during the states of excess energy [22], and the subsequent release of the stored TGs during the states of energy depletion [23]. Dysfunctional adipose tissue, such as in lipodystrophy and obesity, is marked by impaired ability to store lipids, decreased insulin sensitivity and glucose uptake, adipose tissue inflammation, and altered adipokine secretion, which can together precipitate systemic insulin resistance, dyslipidemia, and metabolic disease [24,25].

Given the genetic evidence linking *TRIB1* with multiple features of cardiometabolic disease and to adipocyte biology, and the important roles of adiponectin and adipose tissue in cardiometabolic health, we hypothesized that *TRIB1* in adipose tissue may be contributing to the myriad human genetic associations between the 8q24 locus and cardiometabolic traits. Here, we report the first adipocyte-specific *Trib1* knockout mouse and show that these mice have an overall improved metabolic phenotype with increased plasma adiponectin levels, decreased plasma TG and cholesterol levels, and improved glucose tolerance. Further mechanistic studies reveal that *TRIB1* regulates plasma adiponectin through increased adiponectin production and secretion and *TRIB1* modulates plasma TG clearance through the regulation of adipose tissue-specific LPL activity.

2. MATERIALS AND METHODS

2.1. Animals

The previously reported *Trib1^{fl/fl}* mice [13] and *Rosa26.Trib1* (*Trib1-RosaSTOPfl/-* and *Trib1-RosaSTOPfl/fl*) transgenic mice [14] were bred in-house. *Trib1^{fl/fl}* mice were crossed with *Adipoq-Cre* mice (Jackson Labs stock #010803) to generate *Trib1^{fl/fl}*; *Adipoq-Cre* + mice (*Trib1* adipocyte-specific knockout (*Trib1^{ASKO}*)) and *Trib1^{fl/fl}*; *Adipoq-Cre* - mice (control *Trib1^{fl/fl}*). The mice were bred in a manner such that all *Trib1^{fl/fl}* and *Trib1^{ASKO}* mice were true littermates. The *Trib1^{ASKO}* mice were crossed with *Ldlr* KO mice (Jackson Labs stock #002207) to generate *Trib1^{fl/fl}*; *Adipoq-Cre* +; *Ldlr* KO mice and *Trib1^{fl/fl}*; *Adipoq-Cre* -; *Ldlr* KO mice. Adipose tissue-specific *Trib1* overexpressing transgenic mice were generated by crossing *Rosa26.Trib1* mice with *Adipoq-Cre* mice (Jackson Labs stock #028020). All mice were on the C57BL/6J background. For experiments with less than 8 mice per group ($N < 8$ mice/group), the experiment was repeated in three independent animal cohorts. The mice were fed ad-libitum on a chow diet unless otherwise noted. All experiments were performed when the mice were 8–12 weeks old unless stated otherwise. For fasting/refeeding experiments, the mice were euthanized at 5 pm (fed), at 9 am the next day after 16-h fast (fasted), and after 3-h refeeding (refed). The mice were fasted for 4 h prior to collecting plasma samples, unless stated otherwise. Blood was collected retro-orbitally and spun at 10,000 rpm for 7 min. Fasting cholesterol and TGs were measured via plate assay using the TC and Infinity triglyceride reagents (Fisher TR13421 and TR22421), and the plasma adipokine levels were measured via ELISA (adiponectin: Millipore EZ-MADPK, HMW adiponectin: Alpco Ltd. 47ADPMSE01, leptin: Millipore EZML-82K, resistin: R&D MRSN00). For high-fat diet (HFD) experiments, the mice were placed on 45% kcal HFD (Research Diets D12451) starting at 8–12 weeks of age. Intraperitoneal glucose

tolerance testing was performed in 16-h-fasted mice using 2 g/kg body weight of glucose as described previously [26]. For fasting/refeeding experiments, the mice were fasted overnight for 16 h and then fed ad-libitum with a chow diet for 3 h. To measure *in vivo* TG secretion, plasma triglycerides were measured in 4-h-fasted mice 30, 60, 120, and 180 min after i.p. injection of 1 mg pluronic (P407) per gram mouse body weight.

2.2. FPLC analysis of pooled plasma

Pooled plasma (200 μ l) from gender- and genotype-matched mice was loaded onto a Superose 6 column (GE Healthcare) calibrated with elution buffer (0.15 M NaCl, 1 mM EDTA). The lipoproteins were eluted in a total of 20 mL elution buffer in 0.5 mL fractions at a rate of 0.3 mL/min. The cholesterol and TG content of each fraction was determined by plate assay using the TC and Infinity triglyceride reagents.

2.3. Western blot analysis

Tissues or cells were lysed and homogenized in RIPA buffer supplemented with 1x Halt Protease and Phosphatase inhibitor (Fisher Scientific PI78444). The lysate was clarified via centrifugation at 12,000 $\times g$ for 15 min at 4 °C. Approximately 30 μ g protein was loaded onto 10% bis-tris SDS-PAGE gel and transferred onto a nitrocellulose membrane. The membrane was blocked in 5% milk or BSA (for phospho-protein analysis) and incubated in the appropriate primary antibody overnight (see [supplementary methods](#)). Protein was detected using a secondary HRP-linked antibody and Luminata Classico Western HRP Substrate (Millipore WBLUC0020). To probe membranes, the membranes were incubated in stripping buffer (Fisher Scientific PI21059) for 15 min before reblocking. All western blots were repeated a minimum of three times, with the representative results shown.

2.4. qPCR analysis

RNA from tissues and cells were isolated using the RNeasy Mini kit (Qiagen). cDNA was synthesized using the High-Capacity cDNA Reverse Transcription Kit (Applied Biosystems). qPCR was performed using predesigned Taqman probes from Thermo Fisher Scientific (see [supplementary methods](#)). Gene expression data were normalized to *Gapdh* and presented as fold change relative to the *Trib1^{fl/fl}* control group (exceptions indicated in the figure legend).

2.5. Microscopy

For adipose tissue histology, scWAT samples (<4 mm thick) from *Trib1^{fl/fl}* and *Trib1^{ASKO}* mice were fixed in 4% PFA for 24 h. The tissues were then embedded in paraffin, sectioned at 7 μ m, and H&E stained. For each mouse, 4 sections at 70 μ m intervals were imaged on a Nikon Eclipse Ti microscope with the 40x objective and analyzed using the Adiposoft ImageJ plugin (parameters: minimum diameter = 10 μ m, maximum diameter = 100 μ m). For Oil Red O staining, the cells were fixed in 4% PFA for 15 min and then placed in 0.3% w/v Oil Red O in 60% isopropanol for 30 min. The cells were washed 5X in distilled H₂O and then imaged with the 20x objective.

2.6. RNA-seq of adipocytes and hepatocytes

Eight- to 12-week-old male mice were euthanized and perfused with PBS after a 4-h fast. ScWAT from individual mice were harvested, minced, and then placed in 6 mL digestion media (0.14 U/mL Liberase TM, 50 U/mL DNase I, 20 mg/mL BSA in DMEM) for 1 h at 37 °C, with shaking at 250 rpm. The tissue prep was then filtered through a 100 μ m cell strainer and spun at 300 $\times g$ for 10 min. The floating adipocyte fraction was collected in 1 mL Qiazol, and RNA was isolated using the RNeasy Lipid Tissue Mini Kit (Qiagen). Livers from the same

mice were harvested and homogenized in TRIzol, and RNA was isolated via chloroform extraction. RNA quality was assessed via Bio-Analyzer before being submitted to the core for bulk, paired-end RNA-sequencing (NextSeq 500). Reads were aligned using STAR and featurecounts, and differential expression analysis was performed using the DESeq2 package. Differentially expressed genes ($\text{padj} < 0.050$) were ranked by the signal-to-noise ratio of DESeq2-normalized counts and analyzed by gene set enrichment analysis (GSEA) using the Gene Ontology gene sets (c5.go.v7.2.symbols.gmt) from MSigDB, with gene set size ≤ 200 and 1000 permutations of the gene sets to determine the enrichment score. Cytoscape enrichment plots were constructed from the GSEA results using $\text{FDR} < 0.01$, and a combined coefficient > 0.375 with combined constant 0.5 as described in [27]. Nodes were clustered using the MCL clustering algorithm in the Autoannotate Cytoscape App. Annotations of the clusters were manually curated.

2.7. SVF generation and differentiation

Subcutaneous inguinal fat pads from 3 to 5 mice of the same gender and genotype were combined and minced in digestion buffer (L-15 Leibovitz media, 1.5% BSA, 1% Pen/Strep, 10 U/mL DNaseI, 480 U/mL Hyaluronidase, 0.14 U/mL Liberase TM). Tissue was allowed to dissociate in digestion buffer for 1 h at 37 °C, with shaking at 250 rpm. The tissue prep was then filtered through a 100 μm cell strainer and spun at $300 \times g$, 4 °C, for 10 min. The pellet was saved, washed in 10 mL culture medium (DMEM, 10% FBS, 1% Pen/Strep, 2 mM L-Glut), and then resuspended in 5 mL culture medium supplemented with 1 $\mu\text{g}/\text{mL}$ insulin before seeding. The media were changed every 2–3 days until the cells were $>95\%$ confluent. Differentiation was initiated with a cocktail including 10% FBS, 1% Pen/Strep, 5 $\mu\text{g}/\text{mL}$ insulin, 1 μM Rosiglitazone, 1 μM Dexamethasone, and 250 μM IBMX in DMEM/F12. After 48 h, the cells were maintained in DMEM/F12 supplemented with only 10% FBS, 1% Pen/Strep, 5 $\mu\text{g}/\text{mL}$ insulin, and 1 μM Rosiglitazone. The experiments were started after day 7 of differentiation.

2.8. Global quantitative proteomics of explant secretomics

The mice were euthanized and perfused with PBS before the dissection of subcutaneous adipose tissue fat pads. Then, 50 mg of tissue was placed into 1 mL of warm, serum-free DMEM in a 12-well plate and pinned down with a transwell insert. The media were collected after 6 h, and proteins were precipitated using methanol. The precipitated proteins were identified and quantified by data-independent acquisition (DIA)-based proteomics as described in the [supplementary methods](#).

2.9. Cloning and lentivirus production

Lentiviral constructs for tetracycline-inducible expression of proteins (mTrib1 and eGFP) in adipocytes for overexpression experiments were cloned by first introducing a 3xFlagHA tag at the C-terminal end of each protein. The fusion proteins were then cloned into the pEN-TTMCS entry vector to introduce a tight TRE promoter and subsequently cloned into the pSLIK-neo lentiviral plasmid via Gateway cloning. mTrib1 and eGFP were also cloned into the pLentiCMVPuroDEST lentiviral vector for constitutive overexpression under the CMV promoter.

To produce the virus, 5×10^6 293T cells were seeded in T75 flasks and transfected with 2 μg MD2G, 3 μg Pax2, and 5 μg lentiviral construct with 30 μL Fugene 6 (Promega) the following day. The media were changed the day after transfection, and the viral supernatant was collected and pooled after 24 h and 48 h. The supernatant was filtered through a 0.45 μm filter, aliquoted, and stored at -80 °C until use.

2.10. Adipocyte cell culture

3T3-L1 cells were purchased from ATCC and cultured in DMEM supplemented with 10% FBS, 1 mM sodium pyruvate, and 1% Pen/Strep. The cells were tested for mycoplasma every three months. To differentiate the 3T3-L1 cells to adipocytes, the cells were induced with growth media supplemented with 1 μM dexamethasone, 0.5 mM IBMX, and 1 $\mu\text{g}/\text{mL}$ insulin for 48 h and then maintained in growth media supplemented with only 1 $\mu\text{g}/\text{mL}$ insulin. Stable doxycycline-inducible 3T3-L1 cells were generated by transducing the cells with lentivirus at an MOI ~ 100 , followed by selection with 1.5 $\mu\text{g}/\text{mL}$ puromycin. Conditioned media were collected in OptiMEM I reduced serum media.

2.11. Fluorescent LPL assay

The LPL activity assay was adapted from Basu et al. [28]. Briefly, adipose tissue was minced in 5 μL x mg tissue weight volume in tissue incubation buffer (PBS, 2 mg/mL FA-free BSA, 5 U/mL heparin), incubated for 1 h in a 37 °C shaker, and centrifuged at 3,000 rpm for 15 min at 4 °C. The clarified supernatant was placed in fresh tubes and diluted 1:10 in tissue incubation buffer. Then, 4 μL of lysate was placed in duplicate in a black-walled 96-well plate, and 100 μL reaction buffer (0.15 M NaCl, 20 mM Tris-HCl pH 8.0, 0.0125% Zwittergent, 1.5% FA-free BSA, 0.62 μM EnzChek (Invitrogen E33955)) was added to each well. The reaction was allowed to incubate for 20 min at 37 °C, and was then read at an excitation of 485 and emission of 515. A blank RFU value was subtracted from all the experimental RFU values, and the resulting values were reported.

2.12. Statistics

GraphPad Prism 8 was used to graph data and to perform parametric 2-tailed Student's *t*-tests for comparison between the two groups, and 1- and 2-way ANOVA analyses with multiple corrections were performed for comparison between multiple groups using either Sidak's or Tukey's method as indicated in the figure legends.

2.13. Study approval

All *in vivo* studies described were approved by the Institutional Animal Care and Use Committee at Columbia University and Helmholtz Centre Munich prior to commencement.

3. RESULTS

3.1. Adipocyte-specific Trib1 knockout does not alter body weight

We generated Trib1_ASKO mice by crossing previously described Trib1-floxed (Trib1^{fl/fl}) C57BL/6 mice [13] with transgenic mice expressing Cre recombinase under the adipocyte-specific *Adipoq* promoter. Efficient *Trib1* deletion in the adipose tissue of Trib1_ASKO mice was confirmed by qPCR in subcutaneous white adipose tissue (scWAT) (Figure 1A), gonadal white adipose tissue (gWAT), and brown adipose tissue (BAT) (Figure 1B), and we did not detect any compensatory changes in *Trib2* or *Trib3* expression in scWAT (Figure 1A). Trib1 message was unchanged in other tissues, including the livers (Figure 1B) of Trib1_ASKO mice, confirming the specificity of the model. Chow-fed Trib1_ASKO mice had a similar overall body weight and fat pad mass to Trib1^{fl/fl} mice (Figure 1C,D), and there was no difference in the adipocyte morphology or size as measured by H&E staining and subsequent morphometric analysis (Figure 1E). Similar results were observed in mice fed a 45% kcal HFD for 12 weeks (Figure 1F,G).

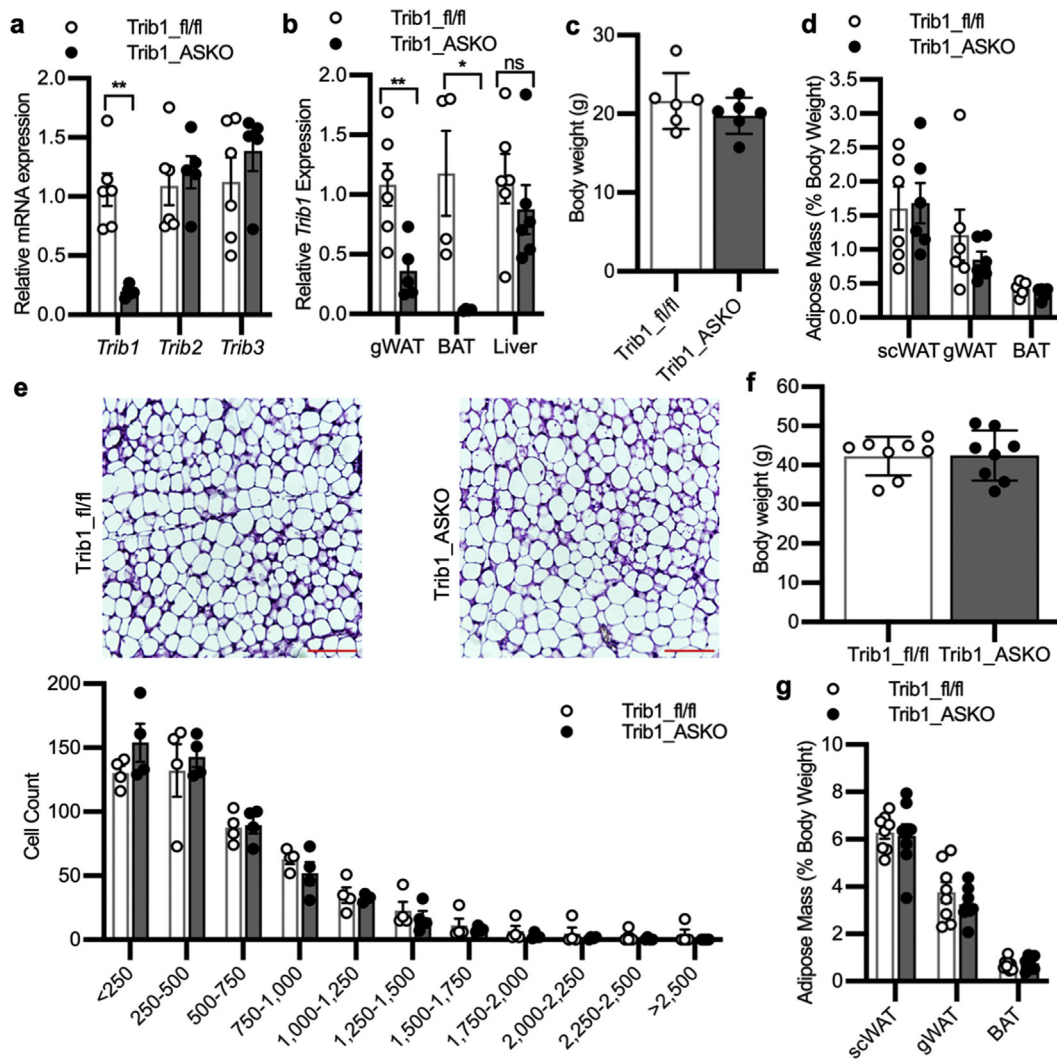


Figure 1: Adipocyte-specific knockout of *Trib1* does not result in defects in adiposity. **A**, Taqman qPCR for *Trib1*, *Trib2*, and *Trib3* in scWAT from 8 to 10-week-old *Trib1*_{fl/fl} and ASKO mice ($n = 5$). **B**, Taqman qPCR for *Trib1* from gWAT ($n = 5$), BAT ($n = 4$), and livers ($n = 6$) from *Trib1*_{fl/fl} and *Trib1*_{ASKO} mice. **C,D**, Body weight (**C**) and adipose tissue depot masses (**D**) in chow-fed *Trib1*_{fl/fl} and ASKO mice ($n = 6$). **E**, Representative H&E stain of scWAT from *Trib1*_{fl/fl} and ASKO mice and quantification of cell size by Adiposoft ($n = 4$ mice). Bar = 100 μ m. **F,G**, Body weight (**F**) and adipose tissue depot masses (**G**) in 12-week-old HFD-fed *Trib1*_{fl/fl} and ASKO mice ($n = 8$). All gene expression data are depicted as the mean \pm s.e.m. All other data are depicted as the mean \pm s.d. Significance in all panels is determined by Student's *t* test (* $p < 0.05$, ** $p < 0.01$).

A previous study reported that *Trib1* haploinsufficiency in mice impairs the upregulation of inflammatory genes in adipose tissue in response to proinflammatory stimuli such as LPS, TNF- α , and HFD feeding [29]. Given the known contribution of adipose tissue inflammation to metabolic disease [30], we checked whether *Trib1*_{ASKO} mice had decreased inflammatory markers in adipose tissue. We measured the inflammatory gene expression in adipose tissue under both chow-fed and HFD-fed conditions and observed no difference between the groups in either diet setting (Figure S2a-c). To investigate the inflammatory response *in vitro*, we treated adipocytes differentiated from the stromal vascular fraction (SVF) from the scWAT of *Trib1*_{fl/fl} and *Trib1*_{ASKO} mice with TNF- α . Similarly, we did not observe any changes in the transcriptional response to TNF- α treatment in SVF-derived adipocytes from *Trib1*_{ASKO} mice compared with *Trib1*_{fl/fl} controls (Figure S2d). These data suggest that the phenotypes we observe in our mice are not due to changes in adipose tissue inflammation.

3.2. *Trib1*_{ASKO} mice have increased plasma adiponectin

Given the association in humans between SNPs near *TRIB1* and plasma adiponectin, we first sought to determine whether *Trib1*_{ASKO} mice had altered circulating adiponectin levels. We found that both male and female *Trib1*_{ASKO} mice on chow diet have significantly increased plasma adiponectin levels compared with their wild-type counterparts, with *Trib1*_{ASKO} males demonstrating a 40% increase (9.92 ng/mL vs. 14.3 ng/mL, $p = 0.014$) and females demonstrating a 20–30% increase (14.4 ng/mL vs. 17.5 ng/mL, $p = 0.027$) (Figure 2A). We also specifically assayed the levels of the high-molecular weight (HMW) form of adiponectin and found this to be increased in *Trib1*_{ASKO} mice as well (Figure 2B). The increase in plasma adiponectin was not accompanied by detectable changes in the adiponectin message levels in the scWAT or gWAT (Figure 2C), suggesting a posttranscriptional role of *TRIB1* in plasma adiponectin regulation. To determine whether *Trib1*_{ASKO} mice had global alterations in adipokine secretion, we investigated the levels of resistin and

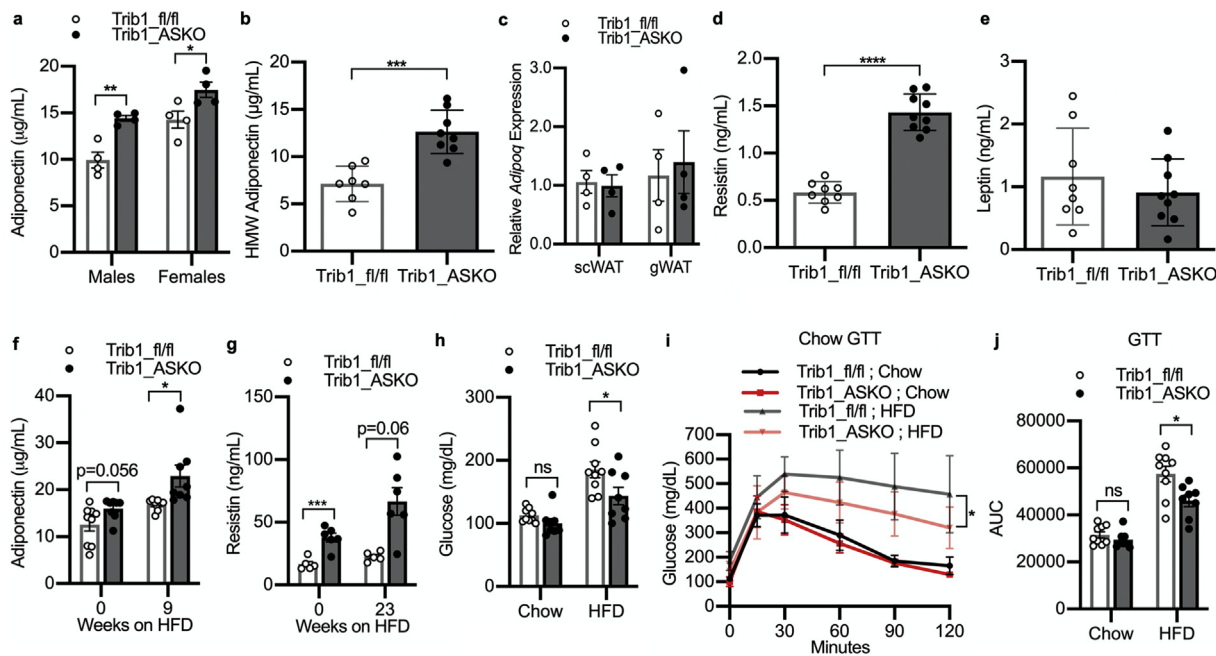


Figure 2: Trib1_ASKO mice have increased plasma adiponectin. **A**, Plasma total adiponectin in 4-h-fasted 8-week-old chow-fed Trib1_{fl/fl} and Trib1_{ASKO} mice ($n = 4$). **B**, Plasma high-molecular weight (HMW) adiponectin in 4-h-fasted 8-week-old chow-fed Trib1_{fl/fl} ($n = 7$) and Trib1_{ASKO} mice ($n = 8$). **C**, Taqman qPCR for *Adipoq* in scWAT and gWAT from Trib1_{fl/fl} and Trib1_{ASKO} mice ($n = 4$). **D,E**, Plasma resistin (**D**) and plasma leptin (**E**) in 4-h-fasted chow-fed Trib1_{fl/fl} and Trib1_{ASKO} mice ($n = 8$). **F**, Plasma adiponectin in 4-h-fasted 9-week-old HFD-fed male Trib1_{fl/fl} and Trib1_{ASKO} mice ($n = 8$). **G**, Plasma resistin in 4-h-fasted 23-week-old HFD-fed male Trib1_{fl/fl} and Trib1_{ASKO} mice ($n = 5$). **H**, Fasting glucose levels after a 16-h overnight fast in chow-fed and 12-week-old HFD-fed male Trib1_{fl/fl} and Trib1_{ASKO} mice ($n = 8$). **I**, Glucose tolerance test in chow-fed and 12-week-old HFD-fed male Trib1_{fl/fl} and Trib1_{ASKO} mice ($n = 8$) after a 16-h overnight fast. **J**, Area-under-the-curve analysis of (**I**). Data on gene expression are presented as mean \pm s.e.m. All other data are presented as mean \pm s.d. The significance in (**I**) was determined by 2-way ANOVA (Sidak's multiple comparisons test). The significance in all other panels was determined by the Student's *t* test (* $p < 0.05$, ** $p < 0.01$, **** $p < 0.0001$).

leptin, two well-studied adipokines in mice. We found that resistin levels were also increased in Trib1_{ASKO} mice (Figure 2D), while plasma levels of leptin were not significantly changed (Figure 2E), demonstrating that Trib1 regulates the secretion of specific adipokines and not global adipokine secretion. Despite increased adiponectin levels, glucose tolerance was not significantly changed in 8–12-week-old chow-fed mice (Figure 2H–J), and SVF-derived adipocytes did not demonstrate increased insulin signaling upon insulin stimulation (Figure S3a). HFD-fed Trib1_{ASKO} mice maintained increased adiponectin levels (Figure 2F) as well as a trend of increased resistin (Figure 2G) compared with wild-type mice. In contrast with chow-fed mice, HFD-fed ASKO mice also had significantly improved glucose tolerance (Figure 2H–J) and decreased fasting plasma insulin levels (Figure S3b) compared with HFD-fed wild-type mice, consistent with improved insulin sensitivity that may be expected in the setting of increased plasma adiponectin levels [16]. Finally, we observed that overnight fasting drastically reduces *Trib1* expression in scWAT, and this reduction is reversed by refeeding of fasted mice (Figure S3c,d). To test whether adipocyte-specific *Trib1* overexpression would result in the opposite phenotype, we inserted *Trib1* in the *Rosa26* locus under the control of the CAG promoter followed by a floxed Stop codon and crossed this mouse with *Adipoq-Cre* mice. *Adipoq-Cre* + mice had 6-fold and 3-fold increased *Trib1* expression in gWAT and scWAT (Figure S4a), respectively. We did not observe significant changes in plasma adiponectin in transgenic mice compared with controls (Figure S4b). However, glucose tolerance was significantly impaired in 8-week-old HFD-fed transgenic mice (Figure S4c,d). In addition, transgenic mice had unaltered plasma cholesterol levels but a modest,

significant increase in plasma triglycerides (Figure S4e,f). Thus, adipocyte-specific knockout and overexpression mouse models confirm the role of adipocyte TRIB1 as a regulator of glucose and lipid homeostasis *in vivo*.

3.3. TRIB1 in adipocytes negatively regulates adiponectin secretion through a proteasome-independent mechanism

Since plasma adiponectin levels were increased in Trib1_{ASKO} mice, we hypothesized that *Trib1* deficiency in adipocytes promotes increased adiponectin secretion. To test this hypothesis, we investigated adiponectin protein expression and secretion in SVF-derived adipocytes from the scWAT of Trib1_{fl/fl} and Trib1_{ASKO} mice. Indeed, consistent with the lack of an adiposity phenotype in the adult mice, SVF-derived adipocytes from Trib1_{fl/fl} and ASKO mice differentiated similarly, as assessed by cellular morphology and lipid accumulation (Figure S5a,b). Importantly, *Trib1* expression in adipocytes derived from ASKO mice was lower relative to adipocytes derived from Trib1_{fl/fl} mice (Figure S5c), demonstrating that *Adipoq-Cre* is efficiently expressed in the *in vitro* setting upon differentiation. As the *AdipoQ-Cre* transgene is only active after adipogenesis has begun, we do not believe that this model can address any potential role for Trib1 in adipogenesis.

Consistent with the observations in whole adipose tissue, adiponectin mRNA expression was unchanged in SVF-derived adipocytes (Figure 3A). However, adiponectin was increased in the conditioned media from adipocytes derived from Trib1_{ASKO} SVF compared with Trib1_{fl/fl} SVF (Figure 3B), confirming increased adiponectin secretion. This was also accompanied by a clear increase in intracellular

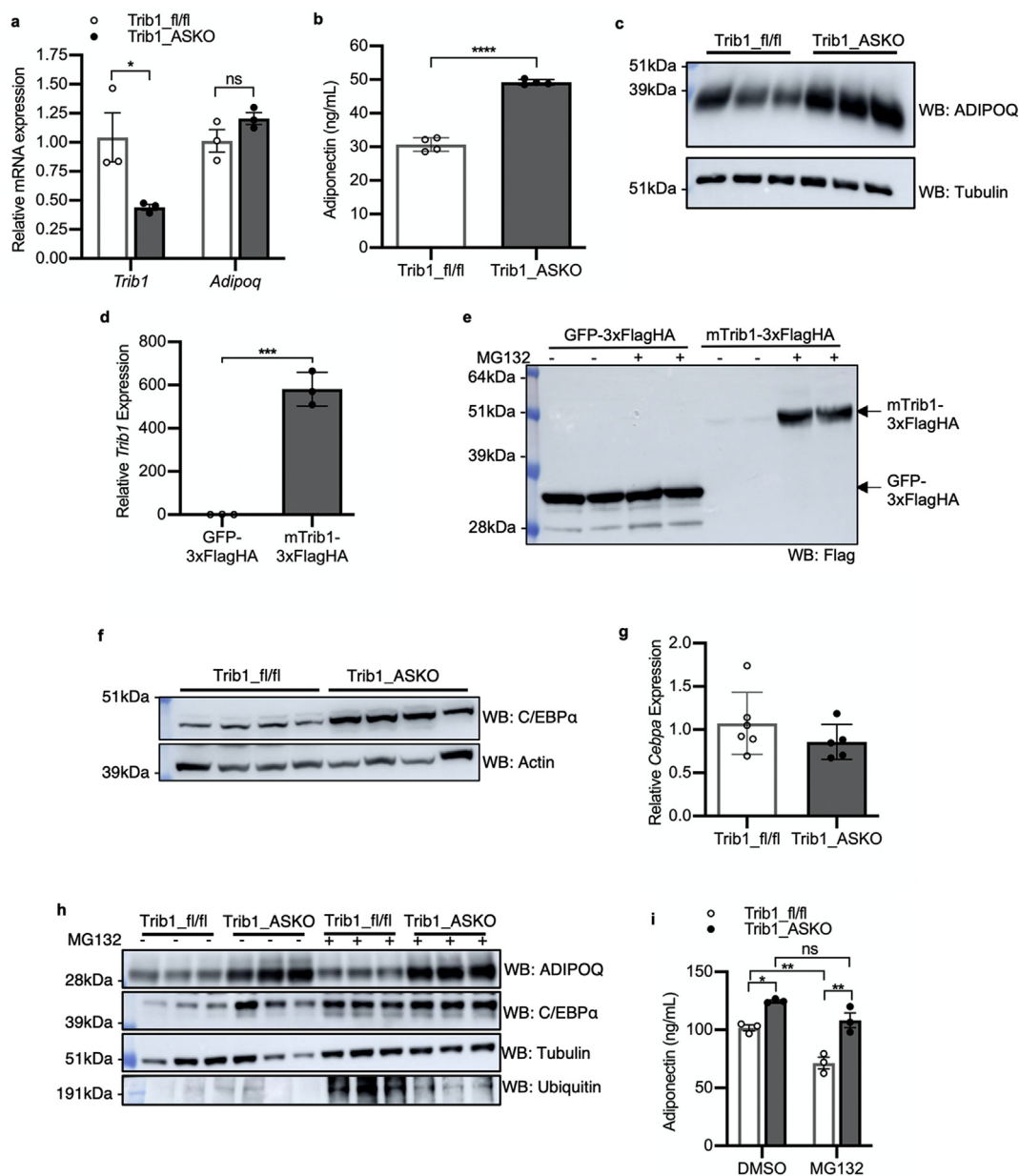


Figure 3: Adipocyte-specific knockout of *Trib1* results in increased adiponectin secretion. **A**, Taqman qPCR for *Trib1* and *Adipoq* in SVF-derived adipocytes ($n = 3$). **B**, Adiponectin concentration in conditioned media from SVF-derived adipocytes ($n = 4$). Conditioned media was generated by culturing SVF-derived adipocytes in OptiMEM reduced-serum media for 4 h. **C**, Western blot analysis of adiponectin (ADIPOQ) in SVF-derived adipocytes. A Western blot of tubulin is shown as a loading control. **D**, Taqman qPCR for *Trib1* in pSlik-neo-TTMCS_eGFP-3xFlagHA and pSlik-neo-TTMCS_mTrib1-3xFlagHA stable 3T3-L1 adipocytes at D14 of differentiation treated with doxycycline (1 $\mu\text{g}/\text{mL}$) for 48 h ($n = 3$). Gene expression is expressed relative to the GFP stable cells. **E**, Western blot for Flag-tagged protein overexpression in pSlik-neo-TTMCS_eGFP-3xFlagHA and pSlik-neo-TTMCS_mTrib1-3xFlagHA stable D14 3T3-L1 adipocytes induced with 1 $\mu\text{g}/\text{mL}$ Dox for 48 h and treated with or without 30 μM MG132 for 5 h. **F**, Western blot of C/EBP α in scWAT from Trib1 fl/fl and Trib1 ASKO mice. A Western blot of actin is shown as a loading control. **G**, qPCR for *Cebpa* gene expression in scWAT from Trib1 fl/fl and Trib1 ASKO mice ($n = 5$). **H, I**, SVF-derived adipocytes from Trib1 fl/fl and Trib1 ASKO scWAT were differentiated, pretreated with 30 μM MG132 for 1 h, and then treated with 30 μM MG132 for an additional 4 h before measuring protein expression and adiponectin secretion. **H**, Western blot for adiponectin (ADIPOQ) and C/EBP α protein in 5-h MG132-treated Trib1 fl/fl and Trib1 ASKO adipocytes. A Western blot of tubulin is shown as a loading control. **I**, ELISA for adiponectin in 4-h conditioned media from 30 μM MG132-treated Trib1 fl/fl and Trib1 ASKO adipocytes ($n = 3$). Data on gene expression are presented as the mean \pm s.e.m. All other data are presented as the mean \pm s.d. The significance in (I) was determined by 2-way ANOVA (Tukey's multiple correction). The significance in all other panels was determined by Student's *t* test (* $p < 0.05$, ** $p < 0.01$, **** $p < 0.0001$).

adiponectin protein levels (Figure 3C), suggesting that increased secretion is in part due to increased cellular adiponectin protein levels, despite the lack of a transcriptional change.

We next investigated whether *Trib1* overexpression in adipocytes would also have an effect on adiponectin secretion and intracellular

protein. We generated a doxycycline-inducible 3xFlagHA-tagged *Trib1* overexpression 3T3-L1 stable cell line that was able to overexpress *Trib1* >500-fold over wild-type values (Figure 3D). We found that TRIB1 protein was barely detectable in these cells via Western blot unless the cells were first treated with the proteasome inhibitor

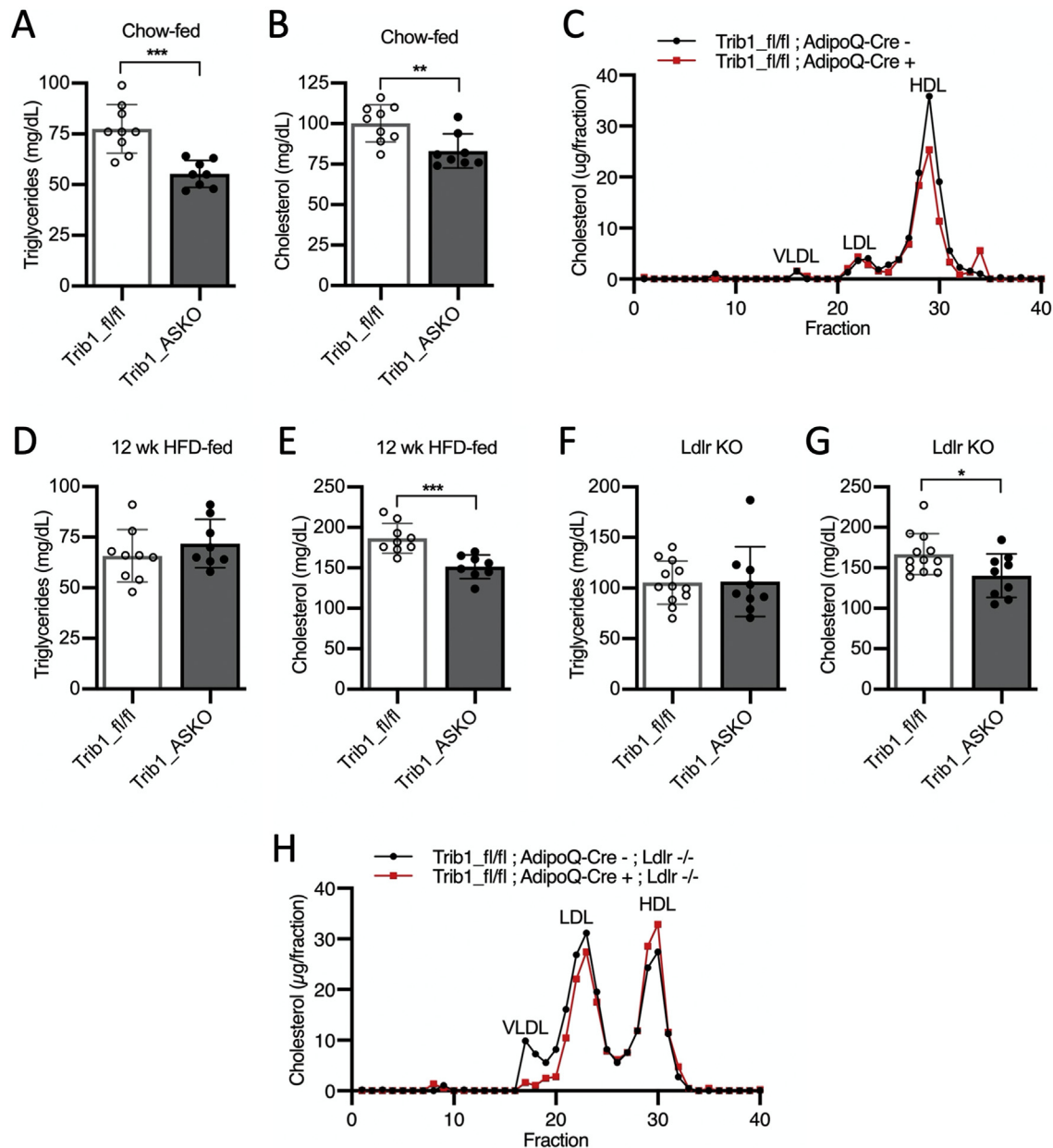


Figure 4: Trib1_{ASKO} mice have decreased plasma cholesterol and triglycerides. **A, B**, Plasma triglyceride (**A**) and total cholesterol (**B**) levels in 8–10-week-old, 4-h-fasted chow-fed male Trib1_{fl/fl} and Trib1_{ASKO} mice ($n = 8$). **C**, Plasma cholesterol FPLC profiles of pooled plasma ($n = 4$) from 4-h-fasted chow-fed male Trib1_{fl/fl} and Trib1_{ASKO} mice. **D, E**, Plasma triglyceride (**D**) and total cholesterol (**E**) levels in 4-h-fasted 12-week-old HFD-fed male Trib1_{fl/fl} and Trib1_{ASKO} mice ($n = 8$). **F, G**, Plasma triglyceride (**F**) and total cholesterol (**G**) levels in 8-week-old, 4-h-fasted chow-fed male Trib1_{fl/fl}; Ldlr KO and Trib1_{ASKO}; Ldlr KO mice ($n = 9$). **H**, Cholesterol FPLC profile of pooled plasma ($n = 3$) from 4-h-fasted chow-fed male Trib1_{fl/fl}; Ldlr KO and Trib1_{ASKO}; Ldlr KO mice. Data are presented as mean \pm s.d. The significance in all the panels are determined by Student's *t* test (* $p < 0.05$, ** $p < 0.01$, *** $p < 0.001$).

MG132, indicating that TRIB1 is unstable and undergoes rapid proteasomal degradation in 3T3-L1 cells (Figure 3E). To avoid differences in the cell-line differentiation capacity caused by selection, we further employed lentiviral delivery of *Trib1* and *eGFP* expressed under the CMV promoter in mature 3T3-L1 adipocytes to assess the effects of *Trib1* overexpression in culture. Despite >60-fold overexpression of *Trib1* via this method, we did not observe any changes in adiponectin secretion or protein levels compared with the GFP control (Figure S6). This is similar to our transgenic mouse data, in which the

overexpression of *Trib1* did not alter the adiponectin levels *in vivo*. Thus, we demonstrate here that TRIB1 protein is highly unstable in adipocytes due to rapid proteasomal degradation.

To better understand the molecular function of TRIB1 in adipose tissue and how it may be regulating adiponectin, we next investigated the previously reported functions of TRIB1 described in other models [13,31]. As a pseudokinase, TRIB1 lacks catalytic phosphorylation activity and is instead understood to function as a scaffolding protein that mediates the interactions between its binding partners [11]. In this

regard, TRIB1 is best known for its role in the proteasomal degradation of the transcription factor C/EBP α via mediating its ubiquitination by the COP1 E3 ubiquitin ligase [31]. In keeping with that function, we found that C/EBP α protein levels were increased in the adipose tissue of Trib1_{ASKO} mice (Figure 3F) without observable changes in the *Cebpa* message levels (Figure 3G). Although C/EBP α is a known transcriptional regulator of adiponectin expression [32], we did not observe a consistent increase in adiponectin expression in either tissue or SVF-derived adipocytes (Figures 2C, 3A), suggesting TRIB1 regulates adiponectin through a mechanism independent of C/EBP α -mediated transcription.

Given TRIB1's role in mediating the ubiquitination of proteins for proteasomal degradation, we further asked whether the proteasome was important in TRIB1's regulation of C/EBP α and adiponectin. We treated Trib1_{ASKO} and Trib1_{fl/fl} SVF-derived adipocytes with MG132 to determine whether proteasomal inhibition would increase C/EBP α and adiponectin protein levels in the control cells but not the KO cells, abrogating the difference in the protein levels between the two. We found that proteasomal inhibition increased C/EBP α protein levels in Trib1_{fl/fl} adipocytes to levels similar to those observed in Trib1_{ASKO} adipocytes (Figure 3H), consistent with the known function of TRIB1 regulating C/EBP α degradation. However, MG132 treatment did not affect adiponectin secretion (Figure 3I) or protein levels (Figure 3H) in the control cells, which indicates that adiponectin levels are not subject to proteasomal regulation, ruling this out as the mechanism through which TRIB1 controls adiponectin levels.

3.4. Adipocyte-specific Trib1 knockout mice have decreased plasma lipids

Since the SNPs in the 8q24 locus significantly associate with both plasma adiponectin and plasma lipids (LDL-C, HDL-C, and TG), we next asked whether adipocyte *Trib1* contributes to plasma lipid regulation. We found that chow-fed Trib1_{ASKO} mice exhibit decreased plasma TG (>28%) and TC (15%) levels compared with their wild-type counterparts (Figure 4A,B), demonstrating the role of adipocyte *Trib1* in plasma lipid regulation. Given that the majority of cholesterol circulates in the HDL fraction in chow-fed C57BL/J mice, FPLC fractionation revealed that the reduced cholesterol in Trib1_{ASKO} mice was reflected in the HDL fraction (Figure 4C). We note that the phenotype of decreased plasma lipids is the opposite direction of effect of the liver-specific knockout of *Trib1*, which results in increased plasma lipids [13], demonstrating opposing tissue-specific roles for TRIB1 in regulating plasma lipids. When placed on HFD for 12 weeks, Trib1_{ASKO} mice no longer exhibited a change in plasma TG compared with Trib1_{fl/fl} littermates (Figure 4D). However, Trib1_{ASKO} mice continued to demonstrate decreased cholesterol levels compared with Trib1_{fl/fl} mice (Figure 4E). As most circulating cholesterol in wildtype C57BL/6 mice is in HDL, we crossed Trib1_{ASKO} mice to LDL receptor knockout mice (Ldlr KO) to determine whether adipocyte TRIB1 alters non-HDL cholesterol. While plasma TGs did not differ between the groups (Figure 4F), we found that Trib1_{ASKO}; Ldlr KO mice on chow diet had reduced TC compared with Trib1_{fl/fl} Ldlr KO mice (Figure 4G), demonstrating that the cholesterol phenotype is at least partially independent of the LDL receptor pathway. Furthermore, we observed decreased VLDL/LDL-C levels on FPLC analysis of pooled plasma from chow-fed Trib1_{ASKO}; Ldlr KO mice relative to Trib1_{fl/fl}; Ldlr KO mice (Figure 4H), showing that loss of adipocyte TRIB1 can alter both LDL-C and HDL-C in a hypercholesterolemic mouse model.

3.5. RNA-sequencing of adipocytes and hepatocytes reveals a primary role for adipose tissue in altered plasma lipid metabolism in Trib1_{ASKO} mice

To understand the mechanism by which adipocyte-specific *Trib1* regulates plasma lipids, we sequenced RNA from adipocytes isolated from the scWAT of Trib1_{fl/fl} and Trib1_{ASKO} mice. Differential expression analysis revealed over 2000 genes that were differentially expressed at a greater than 2-fold change (Figure 5A), emphasizing a widespread role of TRIB1 in adipose tissue. We considered the possibility that altered hepatic metabolism could explain the phenotypes observed in Trib1_{ASKO} mice, given that the liver is a major regulator of lipoprotein metabolism and that adipokines such as adiponectin can signal to the liver [17]. However, RNA-seq of livers from the same mice revealed very few differentially expressed genes, none of which were major lipid regulators (Figure 5B, Table S1). Thus, we concluded that adipocyte TRIB1 is regulating plasma lipids through direct regulation by adipose tissue itself.

We next ranked differentially expressed genes by signal-to-noise ratio in expression and performed GSEA (Figure 5C). Notably, GSEA highlighted a striking enrichment of the mitochondrial genes among the upregulated genes, including genes coding for proteins in the electron transport chain, mitochondrial ribosomes, and the mitochondrial membrane, suggesting a potential role for mitochondria in the phenotypes we observed. Furthermore, multiple gene sets involved in lipid metabolism were upregulated, pointing toward the role of adipocyte-specific *Trib1* in the regulation of lipids through lipid breakdown and metabolism (Dataset S1).

3.6. LPL activity is increased in Trib1_{ASKO} adipose tissue

Given the importance of adipocytes in TG storage, we next sought to identify the physiological mechanism whereby adipocyte-specific knockout of *Trib1* results in reduced plasma TG levels. One mechanism through which adipose tissue contributes to plasma TGs is through the lipolysis of TGs in the lipid droplet and their release as free fatty acids into the bloodstream; subsequently, free fatty acids can be repackaged as TGs and secreted by the liver in the form of VLDL [33]. To assess the effect of *Trib1* deletion in adipose tissue, we first measured plasma nonesterified free fatty acids (NEFA) and glycerol, markers of lipolysis, after stimulating lipolysis by fasting mice overnight for 16 h. We found that NEFA and glycerol levels were comparable between Trib1_{ASKO} and Trib1_{fl/fl} mice after prolonged fasting (Figure S7a,b), indicating that loss of adipocyte *Trib1* does not impact lipolysis rates under stimulation. We also assessed the protein levels of adipose triglyceride lipase (ATGL), the rate-limiting enzyme of triglyceride lipolysis, and the activation of hormone sensitive lipase (HSL), a key lipolytic driver in adipose tissue that is activated by the phosphorylation of key residues [23]. We were unable to detect any differences in the abundance of ATGL or phospho-HSL in subcutaneous adipose tissue from Trib1_{ASKO} and Trib1_{fl/fl} mice (Figure S7c–e). Consistent with these observations, when we treated the mice with poloxamer 407 to inhibit peripheral lipolysis [34], we did not observe a difference in the accumulation of plasma triglycerides, indicating no change in hepatic triglyceride production in Trib1_{ASKO} mice (Figure S7f), indicating that the adipose tissue does not provide significantly different amounts of fatty acids to the liver.

Given the observed changes in plasma adipokine secretion and the importance of adipose endocrine functions, we next performed an unbiased secretomics experiment to identify differentially secreted proteins from Trib1_{ASKO} adipose tissue. We incubated scWAT explant tissue from Trib1_{fl/fl} and Trib1_{ASKO} mice for 6 h in serum-free media and then identified and quantified the proteins in the

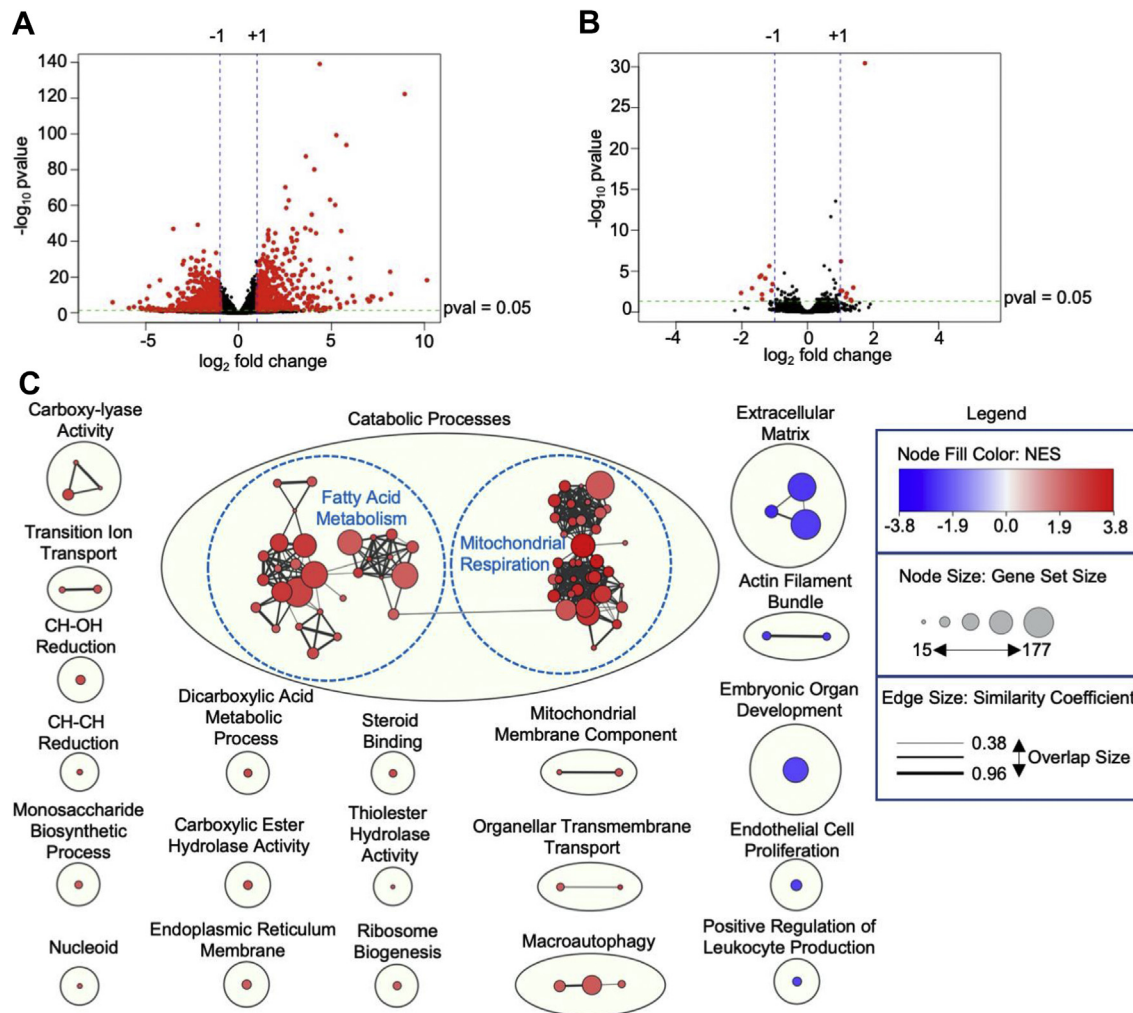


Figure 5: Trib1_ASKO adipocytes have widespread transcriptional changes in mitochondrial and lipid metabolism pathways. **A**, Volcano plot of DESeq2 analysis of RNA-seq data from adipocytes isolated from scWAT from Trib1_{fl/fl} and Trib1_ASKO mice ($n = 4$). **B**, Volcano plot of DESeq2 analysis of RNA-seq data from hepatocytes from Trib1_{fl/fl} and Trib1_ASKO mice ($n = 4$). **C**, Cytoscape enrichment plot of gene set enrichment analysis (GSEA) of differentially expressed adipocyte genes ($\text{padj} < 0.05$). Enrichment analysis and clustering were performed as described in the Methods section. Clusters upregulated in the Trib1_ASKO samples are shown in red, and clusters upregulated in the Trib1_{fl/fl} samples are shown in blue. Dashed blue outlines indicate larger clusters that were further subclustered manually to facilitate interpretation. NES = normalized enrichment score.

conditioned media via data independent acquisition (DIA) (Dataset S2). Consistent with our earlier findings of increased plasma adiponectin and resistin (Figure 2A,D), an increase in adiponectin (>50%) and resistin was found in the conditioned media from the ASKO tissue (Figure 6A), thus validating our secretomics data. Interestingly, we observed significantly decreased ANGPTL4 secretion from Trib1_ASKO scWAT explants (Figure 6A). ANGPTL4 is an inhibitor of LPL, which binds to the endothelium in capillaries and hydrolyzes TGs in circulating lipoproteins to free fatty acids, allowing for their uptake and clearance into tissues, including adipose tissue [35,36]. In addition to changes in secretion, *Angptl4* expression was decreased and *Lpl* expression was increased significantly in our RNA-seq dataset. The expression of *Lmf1*, which codes for the lipase maturation factor and is important for the proper folding and secretion of LPL [37], was also notably increased in ASKO adipocytes (Figure 6B). Overall, these suggest increased LPL activity in ASKO adipose tissue. We next measured LPL activity in adipose tissue extracts from Trib1_{fl/fl} and Trib1_ASKO mice via the cleavage of a fluorescent lipid substrate and found that adipose tissue extracts from both scWAT and gWAT from

Trib1_ASKO mice demonstrated increased lipase activity (Figure 6C,D), likely contributing to increased TG clearance in Trib1_ASKO mice. As BAT LPL activity is also a critical regulator of metabolism, we measured both LPL activity and *Lpl* and *Angptl4* gene expression in Trib1_{fl/fl} and Trib1_ASKO BAT. We observed no changes in LPL activity between mouse groups nor did we observe changes in the gene expression of most key BAT genes (Figure S8a,b).

4. DISCUSSION

GWAS have identified SNPs near the *TRIB1* gene that are significantly associated with plasma lipids, liver enzymes, plasma adiponectin, HbA1c, and CAD [1–6,8,9,15]. Previous studies focusing on hepatic and myeloid TRIB1 have shown various tissue-specific beneficial and detrimental roles of TRIB1 in plasma lipid regulation and CAD as well as in hepatic lipogenesis [12–14]. Here, we report the first adipocyte-specific deletion of *Trib1* in mice and provide the first *in vivo* validation of the association between *Trib1* and adiponectin. In addition, Trib1_ASKO mice exhibit a beneficial metabolic profile that includes

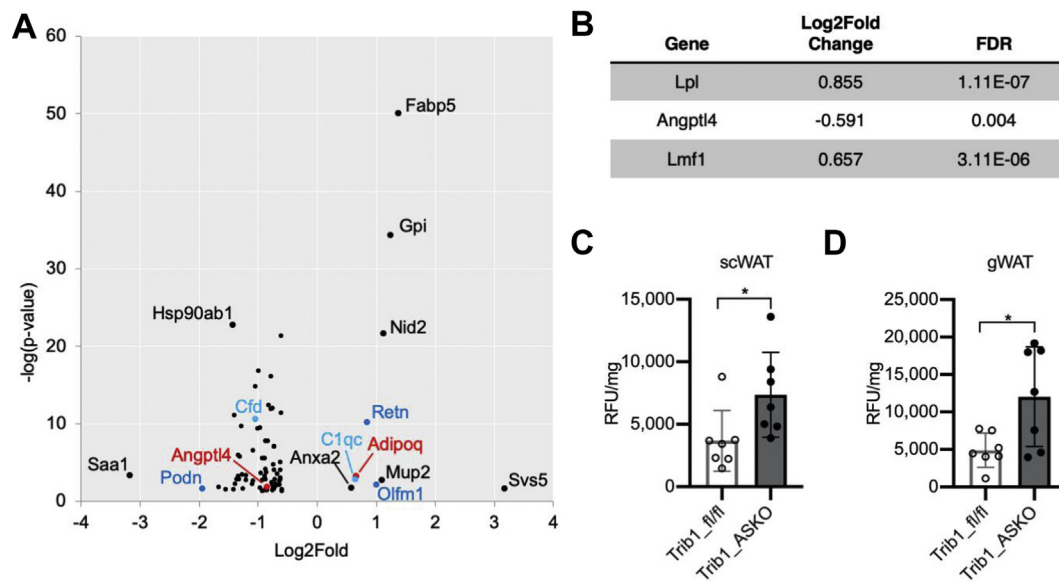


Figure 6: Trib1_ASKO mice exhibit increased adipose tissue lipoprotein lipase activity. **A**, DIA proteomics data of conditioned media from Trib1_ASKO vs. Trib1_fi/fl scWAT explants ($n = 3$). Differential secretion was determined by Spectronaut analysis, and the results were filtered for secreted proteins (Uniprot keywords). Size and color of datapoints are for facilitating visualization. **B**, DESeq2 results for *Lpl*, *Angptl4*, and *Lmf1* from RNA-seq of Trib1_fi/fl and Trib1_ASKO adipocytes. **C,D**, Lpl activity in scWAT (**C**) and gWAT (**D**) from Trib1_fi/fl and Trib1_ASKO mice ($n = 5$). Data are presented as mean \pm s.d. Significance in **C,D** is determined by Student's *t* test (* $p < 0.05$).

elevated adiponectin, improved glucose tolerance, reduced plasma lipids, and increased LPL activity. Interestingly, the reduction in plasma TGs and cholesterol observed in Trib1_ASKO mice is contrary to the finding in previously reported liver-specific knockout mice, which exhibited increased plasma TC and TG [13]. These *in vivo* findings demonstrate that a reduction of adipocyte *TRIB1* has therapeutic potential in the treatment of metabolic disease.

Plasma adiponectin levels are associated with improved metabolic health in both humans [16,18] and mice [38,39], and although studies using recombinant adiponectin in mice have been promising [40], they are challenging due to the complex multimeric structure of adiponectin [21]. Thus, mechanisms that increase endogenous adiponectin may be a more viable approach. Here, we show that inhibiting *TRIB1* in adipocytes results in a robust increase (up to 40%) in circulating adiponectin. The role of adiponectin in insulin sensitization is perhaps its most widely recognized physiological effect [41,42]. We found that HFD-fed ASKO mice have reduced plasma insulin and improved glucose tolerance compared with Trib1_fi/fl mice, consistent with previous studies showing that adiponectin transgenic mice with 2–3-fold increases in circulating adiponectin have improved glucose tolerance [38].

The 8q24 SNPs are associated most strongly with plasma TG in humans [1,2,10]. White adipose tissue is a major contributor to plasma TG regulation due to its ability to clear circulating TGs through LPL or to output FFAs through lipolysis. While chow-fed ASKO mice did not demonstrate changes in the markers of lipolysis, adipose explant secretomics and gene expression profiling revealed increased LPL and decreased ANGPTL4 production in their adipose tissue, and this was accompanied by increased adipose tissue LPL activity in Trib1_ASKO mice. Trib1_ASKO mice also exhibit decreased plasma TG levels, consistent with observations in humans where loss-of-function variants in endogenous inhibitors of LPL such as ANGPTL4, ANGPTL3, and APOC3 are found to be associated with reduced plasma TGs as well as with reduced CAD [43–45]. ANGPTL4 has additionally been found to be positively associated with other markers of the metabolic syndrome

(MetS), including BMI, fasting glucose, and insulin levels [46]. Thus, in addition to regulating plasma TGs, increased LPL activity and decreased ANGPTL4 production may regulate several aspects of metabolic health in ASKO mice.

We also found that Trib1_ASKO mice exhibit decreased plasma TC and LDL-C levels. There is precedent that the observed increase in LPL activity in the Trib1_ASKO mice drives the decrease in plasma cholesterol, as multiple studies using transgenic *Lpl* animal models [47–49] or *Angptl4* knockout or transgenic mice [50,51] demonstrate that increased LPL activity protects from diet-induced hypercholesterolemia and decreases plasma LDL-C levels. Mechanistically, lipolysis-mediated reductions of TGs in VLDL particles have been proposed to facilitate enhanced clearance of the resulting remnant particles via receptors such as the LDLR [52,53]. While further studies are needed to determine whether increased LPL activity is responsible for the reduced plasma lipids in Trib1_ASKO mice, regulation of LPL activity by adipocyte-specific *TRIB1* is a novel finding that deepens our understanding of the mechanisms by which *TRIB1* can contribute to dyslipidemia as suggested by GWAS. These findings also raise the question that through which tissue *Trib1* predominantly affects plasma lipid metabolism. This could be tested in animal models through the deletion of *Trib1* in both hepatocytes and adipocytes in the same animal. However, to answer this question in humans, the understanding of which tissue the GWAS SNPs are functionally relevant in is required, a critical knowledge gap in the field that warrants further attention.

Given the established role of LPL in hydrolyzing circulating triglycerides and allowing for their clearance from circulation into nearby tissues [54], increased LPL activity would be expected to drive increased uptake of plasma TGs into adipocytes in Trib1_ASKO mice. Interestingly, previously reported adipocyte-specific LPL transgenic mice do not display changes in adiposity [49,55], indicating that there are compensatory mechanisms to maintain body weight. Similarly, we did not observe changes in body weight or adiposity in Trib1_ASKO mice despite increased LPL activity. GSEA of our RNA-seq data revealed the

upregulation of genes encoding mitochondrial components, suggestive of increased mitochondrial activity. Notably, the expression of *Ucp1* was unchanged in Trib1_ASKO based on our RNA-seq data, implying that no WAT browning is occurring. A resulting increase in energy expenditure could potentially explain the lack of an adipocyte size phenotype in Trib1_ASKO mice despite increased adipose tissue LPL activity and presumed fatty acid uptake.

Given that adiponectin has many well-studied roles in regulating cardiometabolic traits, including lipid metabolism and coronary artery disease [18,20], an important outstanding question is whether increased adiponectin also contributes to, and perhaps drive, the lipid phenotypes observed in the Trib1_ASKO mice. Experimental evidence indicate that adiponectin plays a role in TG metabolism, as plasma adiponectin correlates with decreased plasma TGs and large VLDL levels and with increased HDL-C in humans [56]. Additionally, adiponectin transgenic mice with 3-fold increased plasma adiponectin levels have increased LPL expression and activity in adipose tissue as well as increased TG clearance [38]. Thus, although the adiponectin phenotype in Trib1_ASKO mice is mild (~20–40% increase) compared with transgenic mouse models, it is possible that the increased adipose tissue LPL activity we observe in Trib1_ASKO mice is secondary to the increased adiponectin levels. The role of adiponectin in plasma cholesterol regulation is less clear. One previous report using transgenic mice with 10-fold increased adiponectin levels found decreased cholesterol in those mice [57]. In humans, epidemiological studies looking at associations between adiponectin and plasma LDL-cholesterol are conflicting or inconclusive [18]. Further studies are required to determine whether the adiponectin phenotype is required for the observed changes in Trib1_ASKO plasma lipids.

TRIB1 is one of three mammalian homologs of the Tribbles pseudo-kinase, which was first discovered in *Drosophila* [11]. These proteins bear homology to serine/threonine kinases, but lack the key catalytic residues that render them unable to catalyze phosphorylation. Instead, they are best understood to function as scaffolding proteins that bring other proteins into proximity with each other to mediate signaling events [11]. One of the best understood molecular functions for TRIB1 is its role in mediating the ubiquitination and degradation of the transcription factor C/EBP α by bringing it into proximity of the COP1 E3 ubiquitin ligase. Tribbles-mediated regulation of C/EBP α protein levels has been shown to be an important function in several models, including as a causal mechanism for the hepatic lipogenesis phenotype in *Trib1* liver-specific knockout mice [13], for myeloid cell proliferation in the context of leukemia [31], and in oogenesis in *Drosophila* [58]. We report here that Trib1_ASKO adipocytes also exhibit increased C/EBP α protein levels in the absence of any change in gene expression, and that C/EBP α protein levels are normalized between control and Trib1_ASKO SVF-derived adipocytes under conditions of proteasomal inhibition. Thus, it appears that adipocyte Trib1 also regulates C/EBP α through proteasomal degradation.

Given the important role of C/EBP α in metabolism and adipocyte differentiation [59], we consider its potential role in the phenotype of the Trib1_ASKO mice. Notably, C/EBP α regulates genes involved in lipid metabolism in adipose tissue and is a known transcriptional regulator of *Lpl* [60,61]. Polymorphisms in C/EBP α have also been found to be associated with plasma TG levels in humans [61]. It is thus possible that increased C/EBP α protein levels in Trib1_ASKO adipose may contribute to the plasma lipid phenotype. C/EBP α is also a known transcriptional regulator of adiponectin [32]. While we have not observed an increase in *Adipoq* gene expression via repeated qPCR measurements in whole adipose tissue, we note that *Adipoq* expression was modestly increased in Trib1_ASKO adipocytes in our RNA-

seq dataset (padj = 0.011, fold change = 1.33). This raises the possibility that increased protein levels of C/EBP α (or a different unknown transcription factor) is driving a small increase in *Adipoq* gene expression that qPCR is not sensitive enough to reliably measure. However, while MG132 treatment of SVF-derived adipocytes increases C/EBP α protein levels, it actually decreases the secretion of adiponectin in wild-type SVF-derived adipocytes (Figure 3). Thus, while TRIB1 certainly appears to regulate C/EBP α in adipose tissue, we propose that this is a separate mechanism from the one governing the Trib1 regulation of adiponectin. One possibility, given the increase in intracellular adiponectin in the absence of increased mRNA or decreased protein degradation, is that Trib1 is regulating the translation of adiponectin, a hypothesis we are currently pursuing among others.

Although C/EBP α is a critical regulator of adipocyte differentiation, we did not observe any differences in adiposity or adipose tissue morphology in Trib1_ASKO mice despite the perturbed C/EBP α protein levels. This could be a result of the *Adipoq* promoter-driven Cre, which is induced late in the process of adipocyte differentiation, thus making our mouse model a post-differentiation knockout of adipocyte TRIB1. A previous report showed that TRIB1 overexpression can inhibit the differentiation of 3T3-L1 cells [62], providing a precedent for the role of Trib1 in adipogenesis. Further studies utilizing a different Cre transgene would be required to determine whether Trib1 plays a similar role in regulating adipogenesis *in vivo*.

5. CONCLUSIONS

In summary, homeostatic control by adipose tissue is crucial to metabolic health, and our study provides evidence that TRIB1 is an important regulator of major adipocyte functions, including the secretion of adiponectin and plasma lipid regulation through LPL. Overall, our studies show that adipocyte-specific *Trib1* is a negative regulator of adiponectin secretion and this appears to be independent of the known function of TRIB1 in promoting proteasomal degradation of C/EBP α . Furthermore, we show that adipocyte-specific *Trib1* regulates plasma lipids in a direction opposite to that of the previously studied liver-specific knockout model and the regulation of TG clearance via adipose tissue LPL in part explains the decreased plasma TG levels in ASKO mice. In contrast to the findings reported for hepatic TRIB1, these data suggest a therapeutically beneficial effect of reduced adipocyte TRIB1 activity in improving multiple aspects of metabolic health and underscore the continued importance of further studies on TRIB1 and the 8q24 GWAS locus.

AUTHOR CONTRIBUTIONS

R.C.B conceived the project, designed the experiments, supervised the analyses, and edited the manuscript. E.E.H. performed the majority of the experiments and data analysis, wrote the first draft of the manuscript, and edited the subsequent versions. G.I.Q helped establish the mouse colony, assisted with SVF isolation, and performed the related molecular biology experiments (i.e. cloning, western blots). R.L. performed western blotting for lipolysis proteins and ELISA analysis. C.X. performed the DESeq2 analysis of the RNA-seq data. A.H. performed the initial FPLC analysis and assisted with all FPLC analyses. K.Y.H performed Western blotting in stable 3T3-L1s and also measured plasma lipids and gene expression in the transgenic mice. C.V.M performed SVF isolation and qPCR work related to the resubmission. R.I. performed SVF isolation and cloning of the viral vectors. J.C. managed the animal colony and assisted with insulin trait experiments.

A.G. designed the transgenic Trib1 mouse and oversaw all the experimental procedures. S.H. and N.S.P. developed the transgenic Trib1 mouse line, while R.A.K. executed the phenotyping of the Trib1 transgenic mice. R.K.S. performed and analyzed the secretomics MS experiment. All the authors read and approved the manuscript.

DATA AVAILABILITY STATEMENT

RNA-seq data will be available from GEO (GSE168596) prior to publication. The full list of the identified proteins and differentially secreted proteins from DIA secretomics (Figure 6A) are available in Dataset S2. Other data that support the findings of this study are available from the corresponding author upon reasonable request.

ACKNOWLEDGMENTS

These studies were funded by R01HL141745 (R.C.B) from the National Heart, Lung, and Blood Institute (NHLBI), Scientific Development Grant 16SDG31180039 (R.C.B) from the American Heart Association, AMPro funding ZT-0026 (S.H.) from the Helmholtz Association, 2020_EKSE.23 (S.H) from the Else Kroner-Fresenius Foundation, and the European Union's Horizon 2020 Marie Slowdowska-Curie Innovative Training Network, TRAIN (project no. 721532) (A.G., N.S.P, S.H, and R.A.K.). In additionally, E.E.H was supported by a Predoctoral F30 NRSA (F30HL146076-01A1) from the NHLBI, and K.Y.H was supported by an institutional T32 (T32DK007328-41A1) from the NIDDK, and A.G and R.A.K were supported with predoctoral funds by the International Helmholtz Research School for Diabetes (Graduate Students call 2019). We thank Adam Linford for his assistance with mouse work.

CONFLICT OF INTEREST

The authors declare no conflict of interest.

APPENDIX A. SUPPLEMENTARY DATA

Supplementary data to this article can be found online at <https://doi.org/10.1016/j.molmet.2021.101412>.

REFERENCES

- Willer, C.J., Sanna, S., Jackson, A.U., Scuteri, A., Bonnycastle, L.L., Clarke, R., et al., 2008. Newly identified loci that influence lipid concentrations and risk of coronary artery disease. *Nature Genetics* 40:161–169.
- Kathiresan, S., Melander, O., Guiducci, C., Surti, A., Burt, N.P., Rieder, M.J., et al., 2008. Six new loci associated with blood low-density lipoprotein cholesterol, high-density lipoprotein cholesterol or triglycerides in humans. *Nature Genetics* 40:189–197.
- Teslovich, T.M., Musunuru, K., Smith, A.V., Edmondson, A.C., Stylianou, I.M., Koseki, M., et al., 2010. Biological, clinical and population relevance of 95 loci for blood lipids. *Nature* 466:707–713.
- Consortium, I.K.C., 2011. Large-scale gene-centric analysis identifies novel variants for coronary artery disease. *PLoS Genetics* 7:e1002260.
- Deloukas, P., Kanoni, S., Willenborg, C., Farrall, M., Assimes, T.L., Thompson, J.R., et al., C.A.D. Consortium, 2013. Large-scale association analysis identifies new risk loci for coronary artery disease. *Nature Genetics* 45:25–33.
- Willer, C.J., Schmidt, E.M., Sengupta, S., Peloso, G.M., Gustafsson, S., Kanoni, S., et al., 2013. Discovery and refinement of loci associated with lipid levels. *Nature Genetics* 45:1274–1283.
- van der Harst, P., Verweij, N., 2018. Identification of 64 novel genetic loci provides an expanded view on the genetic architecture of coronary artery disease. *Circulation Research* 122:433–443.
- Chambers, J.C., Zhang, W., Sehmi, J., Li, X., Wass, M.N., Van der Harst, P., et al., 2011. Genome-wide association study identifies loci influencing concentrations of liver enzymes in plasma. *Nature Genetics* 43:1131–1138.
- Chen, J., Spracklen, C.N., Marenne, G., Varshney, A., Corbin, L.J., Luan, J., et al., 2021. The trans-ancestral genomic architecture of glycemic traits. *Nature Genetics*.
- Jadhav, K.S., Bauer, R.C., 2019. Trouble with tribbles-1. *Arteriosclerosis, Thrombosis, and Vascular Biology* 39:998–1005.
- Eyers, P.A., Keeshan, K., Kannan, N., 2017. Tribbles in the 21st century: the evolving roles of Tribbles pseudokinases in biology and disease. *Trends in Cell Biology* 27:284–298.
- Burkhardt, R., Toh, S.A., Lagor, W.R., Birkeland, A., Levin, M., Li, X., et al., 2010. Trib1 is a lipid- and myocardial infarction-associated gene that regulates hepatic lipogenesis and VLDL production in mice. *Journal of Clinical Investigation* 120:4410–4414.
- Bauer, R.C., Sasaki, M., Cohen, D.M., Cui, J., Smith, M.A., Yenilmez, B.O., et al., 2015. Tribbles-1 regulates hepatic lipogenesis through posttranscriptional regulation of C/EBPalpha. *Journal of Clinical Investigation* 125:3809–3818.
- Johnston, J.M., Angyal, A., Bauer, R.C., Hamby, S., Suvarna, S.K., Baidzajeva, K., et al., 2019. Myeloid Tribbles 1 induces early atherosclerosis via enhanced foam cell expansion. *Science Advances* 5:eaax9183.
- Dastani, Z., Hivert, M.F., Timpson, N., Perry, J.R., Yuan, X., Scott, R.A., et al., 2012. Novel loci for adiponectin levels and their influence on type 2 diabetes and metabolic traits: a multi-ethnic meta-analysis of 45,891 individuals. *PLoS Genetics* 8:e1002607.
- Lihn, A.S., Pedersen, S.B., Richelsen, B., 2005. Adiponectin: action, regulation and association to insulin sensitivity. *Obesity Reviews* 6:13–21.
- Xu, A., Wang, Y., Keshaw, H., Xu, L.Y., Lam, K.S., Cooper, G.J., 2003. The fat-derived hormone adiponectin alleviates alcoholic and nonalcoholic fatty liver diseases in mice. *Journal of Clinical Investigation* 112:91–100.
- Izadi, V., Farabad, E., Azadbakht, L., 2013. Epidemiologic evidence on serum adiponectin level and lipid profile. *International Journal of Preventive Medicine* 4:133–140.
- Pagano, C., Soardo, G., Esposito, W., Fallo, F., Basan, L., Donnini, D., et al., 2005. Plasma adiponectin is decreased in nonalcoholic fatty liver disease. *European Journal of Endocrinology* 152:113–118.
- Pischon, T., Girman, C.J., Hotamisligil, G.S., Rifai, N., Hu, F.B., Rimm, E.B., 2004. Plasma adiponectin levels and risk of myocardial infarction in men. *JAMA* 291:1730–1737.
- Liu, Y., Vu, V., Sweeney, G., 2019. Examining the potential of developing and implementing use of adiponectin-targeted therapeutics for metabolic and cardiovascular diseases. *Frontiers in Endocrinology* 10:842.
- Rosen, E.D., Spiegelman, B.M., 2006. Adipocytes as regulators of energy balance and glucose homeostasis. *Nature* 444:847–853.
- Nielsen, T.S., Jessen, N., Jorgensen, J.O., Moller, N., Lund, S., 2014. Dissecting adipose tissue lipolysis: molecular regulation and implications for metabolic disease. *Journal of Molecular Endocrinology* 52:R199–R222.
- Blüher, M., 2013. Adipose tissue dysfunction contributes to obesity related metabolic diseases. *Best Practice & Research Clinical Endocrinology & Metabolism* 27:163–177.
- Mann, J.P., Savage, D.B., 2019. What lipodystrophies teach us about the metabolic syndrome. *Journal of Clinical Investigation* 129:4009–4021.
- Lagor, W.R., Tong, F., Jarrett, K.E., Lin, W., Conlon, D.M., Smith, M., et al., 2015. Deletion of murine Arv1 results in a lean phenotype with increased energy expenditure. *Nutrition & Diabetes* 5:e181.
- Reimand, J., Isserlin, R., Voisin, V., Kucera, M., Tannus-Lopes, C., Rostamianfar, A., et al., 2019. Pathway enrichment analysis and visualization of omics data using g:Profiler, GSEA, Cytoscape and EnrichmentMap. *Nature Protocols* 14:482–517.
- Basu, D., Manjun, J., Jin, W., 2011. Determination of lipoprotein lipase activity using a novel fluorescent lipase assay. *The Journal of Lipid Research* 52:826–832.

- [29] Ostertag, A., Jones, A., Rose, A.J., Liebert, M., Kleinsorg, S., Reimann, A., et al., 2010. Control of adipose tissue inflammation through TRB1. *Diabetes* 59:1991–2000.
- [30] Shah, A., Mehta, N., Reilly, M.P., 2008. Adipose inflammation, insulin resistance, and cardiovascular disease. *JPEN - Journal of Parenteral and Enteral Nutrition* 32:638–644.
- [31] Dedhia, P.H., Keeshan, K., Uljon, S., Xu, L., Vega, M.E., Shestova, O., et al., 2010. Differential ability of Tribbles family members to promote degradation of C/EBPalpha and induce acute myelogenous leukemia. *Blood* 116:1321–1328.
- [32] Christy, R.J., Yang, V.W., Ntambi, J.M., Geiman, D.E., Landschulz, W.H., Friedman, A.D., et al., 1989. Differentiation-induced gene expression in 3T3-L1 preadipocytes: CCAAT/enhancer binding protein interacts with and activates the promoters of two adipocyte-specific genes. *Genes & Development* 3: 1323–1335.
- [33] Duncan, R.E., Ahmadian, M., Jaworski, K., Sarkadi-Nagy, E., Sul, H.S., 2007. Regulation of lipolysis in adipocytes. *Annual Review of Nutrition* 27:79–101.
- [34] Millar, J.S., Cromley, D.A., McCoy, M.G., Rader, D.J., Billheimer, J.T., 2005. Determining hepatic triglyceride production in mice: comparison of poloxamer 407 with Triton WR-1339. *The Journal of Lipid Research* 46:2023–2028.
- [35] Dijk, W., Kersten, S., 2014. Regulation of lipoprotein lipase by Angptl4. *Trends in Endocrinology and Metabolism* 25:146–155.
- [36] Goldberg, I.J., Merkel, M., 2001. Lipoprotein lipase: physiology, biochemistry, and molecular biology. *Frontiers in Bioscience* 6:D388–D405.
- [37] Doolittle, M.H., Ehrhardt, N., Peterfy, M., 2010. Lipase maturation factor 1: structure and role in lipase folding and assembly. *Current Opinion in Lipidology* 21:198–203.
- [38] Combs, T.P., Pajvani, U.B., Berg, A.H., Lin, Y., Jelicks, L.A., Laplante, M., et al., 2004. A transgenic mouse with a deletion in the collagenous domain of adiponectin displays elevated circulating adiponectin and improved insulin sensitivity. *Endocrinology* 145:367–383.
- [39] Xia, J.Y., Sun, K., Hepler, C., Ghaben, A.L., Gupta, R.K., An, Y.A., et al., 2018. Acute loss of adipose tissue-derived adiponectin triggers immediate metabolic deterioration in mice. *Diabetologia* 61:932–941.
- [40] Berg, A.H., Combs, T.P., Du, X., Brownlee, M., Scherer, P.E., 2001. The adipocyte-secreted protein Acrp30 enhances hepatic insulin action. *Nature Medicine* 7:947–953.
- [41] Tilg, H., Moschen, A.R., 2006. Adipocytokines: mediators linking adipose tissue, inflammation and immunity. *Nature Reviews Immunology* 6:772–783.
- [42] Yanai, H., Yoshida, H., 2019. Beneficial effects of adiponectin on glucose and lipid metabolism and atherosclerotic progression: mechanisms and perspectives. *International Journal of Molecular Sciences* 20.
- [43] Dewey, F.E., Gusarova, V., O'Dushlaine, C., Gottesman, O., Trejos, J., Hunt, C., et al., 2016. Inactivating variants in ANGPTL4 and risk of coronary artery disease. *New England Journal of Medicine* 374:1123–1133.
- [44] Tall, A.R., 2017. Increasing lipolysis and reducing atherosclerosis. *New England Journal of Medicine* 377:280–283.
- [45] Crosby, J., Peloso, G.M., Auer, P.L., Crosslin, D.R., Stitzel, N.O., Lange, L.A., et al., TG and HDL Working Group of the Exome Sequencing Project, 2014. Loss-of-function mutations in APOC3, triglycerides, and coronary disease. *New England Journal of Medicine* 371:22–31.
- [46] Mehta, N., Qamar, A., Qu, L., Qasim, A.N., Mehta, N.N., Reilly, M.P., et al., 2014. Differential association of plasma angiopoietin-like proteins 3 and 4 with lipid and metabolic traits. *Arteriosclerosis, Thrombosis, and Vascular Biology* 34:1057–1063.
- [47] Shimada, M., Ishibashi, S., Inaba, T., Yagyu, H., Harada, K., Osuga, J.I., et al., 1996. Suppression of diet-induced atherosclerosis in low density lipoprotein receptor knockout mice overexpressing lipoprotein lipase. *Proceedings of the National Academy of Sciences of the U S A* 93:7242–7246.
- [48] Fan, J., Unoki, H., Kojima, N., Sun, H., Shimoyamada, H., Deng, H., et al., 2001. Overexpression of lipoprotein lipase in transgenic rabbits inhibits diet-induced hypercholesterolemia and atherosclerosis. *Journal of Biological Chemistry* 276:40071–40079.
- [49] Walton, R.G., Zhu, B., Unal, R., Spencer, M., Sunkara, M., Morris, A.J., et al., 2015. Increasing adipocyte lipoprotein lipase improves glucose metabolism in high fat diet-induced obesity. *Journal of Biological Chemistry* 290:11547–11556.
- [50] Koster, A., Chao, Y.B., Mosior, M., Ford, A., Gonzalez-DeWhitt, P.A., Hale, J.E., et al., 2005. Transgenic angiopoietin-like (angptl)4 overexpression and targeted disruption of angptl4 and angptl3: regulation of triglyceride metabolism. *Endocrinology* 146:4943–4950.
- [51] Aryal, B., Singh, A.K., Zhang, X., Varela, L., Rotllan, N., Goedeke, L., et al., 2018. Absence of ANGPTL4 in adipose tissue improves glucose tolerance and attenuates atherogenesis. *JCI Insight* 3.
- [52] Aviram, M., Bierman, E.L., Chait, A., 1988. Modification of low density lipoprotein by lipoprotein lipase or hepatic lipase induces enhanced uptake and cholesterol accumulation in cells. *Journal of Biological Chemistry* 263:15416–15422.
- [53] Sehayek, E., Lewin-Velvet, U., Chajek-Shaul, T., Eisenberg, S., 1991. Lipolysis exposes unreactive endogenous apolipoprotein E-3 in human and rat plasma very low density lipoprotein. *Journal of Clinical Investigation* 88:553–560.
- [54] Goldberg, I.J., Eckel, R.H., Abumrad, N.A., 2009. Regulation of fatty acid uptake into tissues: lipoprotein lipase- and CD36-mediated pathways. *The Journal of Lipid Research* 50(Suppl):S86–S90.
- [55] Hensley, L.L., Ranganathan, G., Wagner, E.M., Wells, B.D., Daniel, J.C., Vu, D., et al., 2003. Transgenic mice expressing lipoprotein lipase in adipose tissue. Absence of the proximal 3'-untranslated region causes translational upregulation. *Journal of Biological Chemistry* 278:32702–32709.
- [56] Christou, G.A., Kiortsis, D.N., 2013. Adiponectin and lipoprotein metabolism. *Obesity Reviews* 14:939–949.
- [57] Bauche, I.B., El Mkadem, S.A., Pottier, A.M., Senou, M., Many, M.C., Rezsóhazy, R., et al., 2007. Overexpression of adiponectin targeted to adipose tissue in transgenic mice: impaired adipocyte differentiation. *Endocrinology* 148:1539–1549.
- [58] Rorth, P., Szabo, K., Texido, G., 2000. The level of C/EBP protein is critical for cell migration during Drosophila oogenesis and is tightly controlled by regulated degradation. *Molecular Cell* 6:23–30.
- [59] Farmer, S.R., 2006. Transcriptional control of adipocyte formation. *Cell Metabolism* 4:263–273.
- [60] Madsen, M.S., Siersbaek, R., Boergesen, M., Nielsen, R., Mandrup, S., 2014. Peroxisome proliferator-activated receptor gamma and C/EBPalpha synergistically activate key metabolic adipocyte genes by assisted loading. *Molecular and Cellular Biology* 34:939–954.
- [61] Olofsson, L.E., Orho-Melander, M., William-Olsson, L., Sjöholm, K., Sjöström, L., Groop, L., et al., 2008. CCAAT/enhancer binding protein alpha (C/EBPalpha) in adipose tissue regulates genes in lipid and glucose metabolism and a genetic variation in C/EBPalpha is associated with serum levels of triglycerides. *Journal of Clinical Endocrinology & Metabolism* 93:4880–4886.
- [62] Naiki, T., Saijou, E., Miyaoka, Y., Sekine, K., Miyajima, A., 2007. TRB2, a mouse Tribbles ortholog, suppresses adipocyte differentiation by inhibiting AKT and C/EBPbeta. *Journal of Biological Chemistry* 282:24075–24082.